Development of safe and effective bacteriophage-mediated therapies against *C. difficile* infections – a proof-of-concept preclinical study

Torben Sølbeck Rasmussen[1*], Sarah Forster[1], Sabina Birgitte Larsen[1], Alexandra Von Münchow[2], Kaare Dyekær Tranæs[1], Anders Brunse[3], Josue Leonardo Castro Mejia[1], Signe Adamberg[4], Axel Kornerup Hansen[2], Kaarel Adamberg[4,5], Camilla Hartmann Friis Hansen[2], Dennis Sandris Nielsen[1*]

[1] Section of Microbiology and Fermentation, Dept. of Food Science, University of Copenhagen, Frederiksberg, Denmark

[2] Section of Experimental Animal Models, Dept. of Veterinary and Animal Sciences, University of Copenhagen, Frederiksberg, Denmark

[3] Section of Comparative Pediatrics and Nutrition, Department of Veterinary and Animal Sciences, University of Copenhagen, Frederiksberg, Denmark

[4] Department of Chemistry and Biotechnology, Tallinn University of Technology, Tallinn, Estonia

[5] Center of Food and Fermentation Technologies, Tallinn, Estonia

*Corresponding author. Email: dn@food.ku.dk / torben@food.ku.dk

Summary: Fecal viromes depleted of enveloped viruses efficiently treat *Clostridioides difficile*-associated diarrhea in a murine model.

ABSTRACT

Fecal microbiota transplantation (FMT) from a healthy donor to recurrent *C. difficile* infection (CDI) patients has proven efficient in curing the disease, possibly through bacteriophage-mediated (phages) modulation of the gut microbiome landscape. Fecal virome transplantation (FVT, sterile filtrated donor feces) has also been shown efficient for treating the disease. FVT has the advantage over FMT that no bacteria are transferred, but FVT does not exclude the risk of transferring eukaryotic viruses. We aimed to develop methodologies to obtain safer FVT by removing and/or inactivating eukaryotic viruses, while maintaining an active phage community. Donor feces were used as inoculum for a chemostat-fermentation to remove eukaryotic viruses by dilution (FVT-ChP). FVT solutions underwent solvent-detergent treatment to inactivate enveloped viruses (FVT-SDT) and pyronin-Y treatment to block the replication of RNA-viruses (FVT-PyT). The efficacy of these treatments was assessed in a CDI mouse model and compared with untreated FVT (FVT-UnT), FMT, and saline-treatment as controls. Intriguingly, 8/8 mice receiving FVT-SDT did not reach the humane endpoints until planned euthanization and expressed limited symptoms of CDI. While 5/7 saline treated mice reached the humane endpoint. Compared to the saline treatment, lower *C. difficile* abundance ($p<0.005$) in the FVT-SDT-treated mice suggested that the intervention had hampered *C. difficile* colonization. The mice receiving FVT-ChP and FVT-UnT tended to express alleviated CDI symptoms compared to the saline control. This proof-of-concept study may constitute the initial step of developing therapeutic tools that targets a broad spectrum of gut-related diseases and thereby substituting FMT with a safer phage-mediated therapies.

INTRODUCTION

During the last decade, it has become evident that a range of diseases is associated with gut microbiome (GM) dysbiosis, including recurrent *Clostridioides difficile* infections (rCDI) *(1–3)*. Fecal microbiota transplantation (FMT) from a healthy donor to rCDI patients has proven very efficient in curing the disease (success rate > 90%) *(4)*. However, FMT still represents safety issues since no screening methods can definitively exclude transfer of adverse effects from the donor *(3)*, as emphasized (June 2019) where two patients in the United States had severe bacterial infections following FMT, of which one patient died *(5)*. Ott et al. *(3)* successfully treated rCDI patients with sterile filtrated donor feces (containing viruses but no intact bacteria). An approach we will refer to as fecal virome transplantation (FVT) in the following. The efficiency of the FVT treatment was similar to FMT (containing bacteria etc.) *(3)*, thus suggesting that the virome plays a decisive role in rCDI treatment with FMT. Another independent clinical study confirmed the efficacy of FVT in treating CDI *(6)*. Most of the gut virome is represented by bacteriophages (phages) that are bacterial viruses that infect in a host-specific manner *(7)*. The concept of applying FVT from a healthy phenotype to a symptomatic phenotype has been further investigated in preclinical studies. Amongst others, Draper et al. showed that FVT affected the murine GM composition after initial perturbation with antibiotics *(8)*, symptoms of type-2-diabetes mellitus in a diet-induced obesity murine model were alleviated after FVT treatment *(9)*, and FVT prevented the development of necrotizing enterocolitis in a preterm piglet model *(10)*. FVT from *Akkermansia muciniphila*-rich donors have also been shown to improve proliferation of commensal gut *A. muciniphila* in healthy recipient mice *(11)*. FVT has the advantage over FMT that no bacteria are transferred. Still, the sterile filtration (normally using 0.45 µm filters) used for FVT does not exclude the obvious risk of transferring eukaryotic viruses. It is possible to screen donor feces for known pathogenic viruses, but during recent years it has become evident that the human gastrointestinal tract harbors hundreds of eukaryotic viruses of unknown function *(7, 12, 13)*. Most likely, many of these viruses are harmless for the human host. Still, it cannot be ruled out that they might play a role in later disease development, as exemplified by the human papillomavirus, a risk factor for cervical cancer years after infection *(14)*. Thus, there is good reason to reduce the transfer of eukaryotic viruses when using FVT to alleviate gut dysbiosis-associated conditions, especially if treating young and/or immune system impaired subjects. Phages do not infect eukaryotic cells and are thought to be a driving agent for a successful FMT/FVT targeting gut-related diseases *(3, 9, 10, 15)*. Phage

therapy has been applied for almost a century *(16)* and is generally considered safe since severe adverse effects are extremely rare *(17–20)*. FMT and FVT have the potential to revolutionize treatments for numerous gut-related diseases, but due to their inherent safety issues, widespread use is unlikely. We therefore aimed to develop methodologies to process a safer FVT by either removing the eukaryotic viruses by dilution (chemostat propagated donor virome) or chemical inactivation (solvent/detergent or pyronin Y) of the eukaryotic viral component, while maintaining an active phageome. Following an efficacy assessment of these processed FVT viromes using a murine CDI model. This proof-of-concept study may constitute the initial step of developing a therapeutic tool targeting a broad spectrum of gut-related diseases, thereby replacing FMT with a safer phage-mediated therapy.

RESULTS

Here we aimed to improve the safety of fecal virome transplantation (FVT) while maintaining treatment efficacy. We developed methodologies that utilized the fundamental differences in characteristics between eukaryotic viruses and phages; the majority of eukaryotic viruses are enveloped RNA viruses *(21–23)* and require eukaryotic hosts for replication, while the majority of phages are non-enveloped DNA viruses *(23, 24)* and require bacterial hosts for replication. A solvent/detergent method was applied to inactivate enveloped viruses (FVT-SDT), pyronin Y was used to inhibit replication of RNA viruses (FVT-PyT), and a chemostat propagated virome (FVT-ChP) was created to remove the majority of eukaryotic viruses by dilution *(25)*. These differently treated viromes were compared with a saline solution, fecal microbiota transplantation (FMT), and untreated donor-filtrated feces (FVT-UnT). All originating from the same intestinal donor material. The safety and efficacy of these treatments were assessed in a *C. difficile* infection mouse model using C57BL/6J mice.

Solvent/detergent treatment inactive an enveloped phage and pyronin Y inhibits replication of RNA phages

The different methodology's ability to differentiate eukaryotic viruses from phages were initially evaluated. Phages representing different characteristics, such as enveloped (phi6) vs. non-enveloped (phiX174, T4, and C2) structure and ss/dsDNA (phiX174, T4, C2) vs. ss/dsRNA (phi6, MS2) based genomes were included in this study to evaluate if their associated plaque forming unit per mL (PFU/mL) was affected after treatment with solvent/detergent or pyronin Y (Fig. 1A

& 1B). The solvent/detergent treatment was expected to inactivate enveloped viruses by dissolving the lipid membrane. The solvent/detergent treatment completely (detection limit = 10 PFU/mL) inactivated the activity of the enveloped phage phi6, while the PFU/mL of the non-enveloped phages phiX174 and T4 was unaffected, while phage C2 showed a 1-log PFU/mL decrease after the solvent/detergent treatment (Fig. 1A). Pyronin Y was intended to inactivate replication of viral RNA genomes. Based on numerous combinations of pyronin Y concentrations, temperatures, and incubation time, an overnight incubation at 40°C with 100 µM pyronin Y was chosen. Although both RNA and DNA viruses were affected by the treatment (Fig. 1B). The pyronin Y treatment decreased the PFU/mL of MS2 (ssRNA genome) with 5 log at 40°C, and decreased the PFU/mL of phage phi6 with more than 4 log at 20°C. While the temperature of 40°C by itself completely inactivated phage phi6. The PFU/mL of phage C2 (dsDNA), phage T4 (dsDNA), and phiX174 (ssDNA) was also affected by the pyronin Y treatment at 40°C, with a decrease of, respectively, 1, 2.5, and 5 log PFU/mL (Fig. 1B). As hypothesized, the pyronin Y treatment did indeed inactivate RNA phages. However, an efficient differentiation of DNA and RNA phages could not be obtained. Analysis of the chemostat propagated fecal-like virome is accounted for in another publication, that showed efficient dilution of eukaryotic viruses *(25)*.

Fecal viromes maintained treatment efficacy after inactivation of enveloped viruses

The survival rate associated with the different treatments was evaluated by a Kaplan-Meier estimate (Fig. 2A) and compared to the saline treated mice (2/7 mice, control). The analysis showed a significantly increased survival rate (8/8 mice, $p = 0.004$) for mice treated with FVT-SDT, while FVT-UnT tended to have improved the survival rate (5/7 mice, $p = 0.067$) compared to control. In contrast, the FVT-PyT treated mice, and unexpectedly, the FMT treatment showed no improvement in survival rate (respectively, 1/8 and 3/8 mice). The effect of FVT-ChP on the survival rate (5/8 mice, $p = 0.235$) was ambiguous. The pathological score of the cecum tissue supported the observed survival rate, where FVT-UnT, -ChP, and -SDT treated mice showed a significant decrease ($p < 0.05$) in pathological score compared with the control mice (Fig. 2B). The concentration of 10 pro- and anti-inflammatory cytokines was also measured in the cecum tissue to support the cecum histology score and to validate the qualitative health evaluation (Fig. S1). The cytokine profiles reflected in general whether the mice survived (i.e. not reaching the humane endpoint) until study termination (low or no inflammatory response) or if they were euthanized (high inflammatory response) due to *C. difficile* infection (Fig. 2C-L). Overall, the

FVT-SDT treatment (inactivation of enveloped viruses) prevented severe *C. difficile* infection and thereby significantly increased the chances of survival. The average pathological score of the saline treatment at 6.7 was similar to the original published CDI mouse model with a pathological score at 7.0 compared to a negative control with a score at 1.3 *(26)*. Hence, reflecting the relative mild symptoms and pathological scores of 2.5 – 3.0 that were associated to the FVT-UnT, -ChP, or -SDT treated mice.

Effective treatments hamper *C. difficile* colonization and thereby disease development

The *C. difficile* abundance was quantified in feces by qPCR to gain a measure of the level of *C. difficile* colonization (Fig. 3A-3C). No *C. difficile* was detected with the qPCR analysis before being inoculated with *C. difficile* (Fig. 3A). The FVT-SDT-treated mice had an average of 2 $\log_{10}$ lower ($p < 0.005$) of *C. difficile* abundance compared to the saline treated mice (Fig. 3B) before the 2nd treatment, while the FVT-UnT and FVT-ChP were 1.5 $\log_{10}$ lower. Suggesting that these three treatments had limited the *C. difficile* gut colonization. In contrast, the FMT and FVT-PyT treated mice had similar *C. difficile* abundance as the saline group. At termination, 7 out of 8 FVT-SDT treated mice tested negative for *C. difficile*, which indicated a clearing of *C. difficile* colonization, whereas all other treatments showed *C. difficile* persistence at termination (Fig. 3C). Also, the levels of the *C. difficile*-associated toxin A/B were measured with an ELISA based assay and showed similar patterns as the qPCR data (Fig. 3D-3F), where the toxin A/B levels in the FVT-SDT treated mice were significant ($p < 0.05$) lower than the saline group (Fig. 3E) and only detected in 2 mice in the FVT-SDT group before the 2nd treatment. Toxin A/B could not be detected at termination in any of the FVT-SDT treated mice (Fig. 3F). The decrease in *C. difficile* abundance (Fig. 3A-3C) and low levels of toxin A/B (Fig. 3D-3F) in the FVT-SDT, FVT-UnT, FVT-ChP treated mice support the phenotypic data of survival rate, histology, and cytokine profile (Fig. 2).

The solvent/detergent treated fecal virome catalyzes an efficient restoration of the bacterial community in a dysbiotic GM

There were no initial differences in bacterial and viral GM profiles at both baseline and before *C. difficile* infection between the mice that later either were euthanized or survived the *C. difficile* infection (Fig. S2, S3, S4, & S5). Importantly, the antibiotic intake through the drinking water was similar between the cages (Table S1). The bacterial taxonomic profile of the mice that were euthanized due to the health status reaching the humane endpoint were all dominated by the genera of *Escherichia/Shigella*, *Enterococcus*, *Clostridioides*, *Bacteroides*, and *Parabacteroides* (Fig. 4C,

4D, & Fig. S6), and this bacterial composition and diversity were significantly ($q < 0.003$) different to the mice that had survived the infection (Fig. 4A & 4B). As an exception, the FMT treated mice that survived the infection appeared with bacterial taxa which overlapped (*Clostridium sensu stricto* and *Ruminococcaceae*) with the taxa present in the FMT inoculum, thereby suggesting that these bacteria had colonized the gut of the FMT treated mice (Fig. 4C & 4D). Two mice treated with FVT-PyT were also colonized with 5 – 20% relative abundance of *Salmonella* spp., which may have accelerated the disease severity. The bacterial taxonomic profile of the mice that had survived the infection were dominated by the taxa of *Lactobacillus*, *Bacteroides*, *Lachnospiraceae, Bifidobacterium*, *Akkermansia*, *Porphyromonadaceaea*, *Bacteroidales*, and *Turibacter,* which also were the dominating taxa in the mice at baseline (Fig. 4C, 4D, & Fig. S6A). This suggests that the GM profile of the mice that survived the *C. difficile* infection was restored into a composition that resembled the GM profile of healthy mice before antibiotic treatment and *C. difficile* infection (baseline). The FVT-SDT treatment possibly improved the chances of restoring the GM composition after the antibiotic treatment, and thereby impacted the mice's chances to fight off the *C. difficile* infection. Also, the viral diversity and composition were significantly ($q < 0.005$) different between the euthanized and surviving mice (Fig. 5A & 5B), where the euthanized mice were characterized by a significant ($p < 0.05$) increase in the relative abundance of the viral order *Petitvirales* and phages that were predicted to target the bacterial genera *Sutterella*. On the contrary, mice that survived the infection until termination were characterized by a significant increase ($p < 0.05$) in the viral order *Caudovirales* as well as phages predicted to target bacterial genera of *Parabacteroides, Bacteroides, Prevotella, Odorifactor*, and *Escherichia* (Fig. S6B & S6C) compared euthanized mice. The eukaryotic viral profile was similar between the different FVT inoculates (Fig. S7) and constituted 0.3 – 2.5% of the total relative abundance (Fig. S8). Importantly, the viral taxonomic resolution was insufficient to differentiate the treatments or outcomes in relation to the relative abundance of eukaryotic viruses (Fig. S7).

DISCUSSION

Here we developed methodologies to mitigate the potential safety issues represented by the eukaryotic viral component in fecal viromes transplantations (FVT) and assessed whether the treatment efficacy against *C. difficile* infection (CDI) *(3, 6)* was maintained in the modified FVTs using a murine CDI model. The fecal eukaryotic viruses were reduced in abundance by dilution in a chemostat setup that selected for phage propagation *(25)* (FVT-ChP) or were inactivated either

by dissolving the lipid membrane of enveloped viruses (FVT-SDT) or by chemical interactions with viral RNA genomes (FVT-PyT). The different modified FVTs were compared with an untreated fecal virome (FVT-UnT), fecal microbiota transplantation (FMT), and a saline (control) solution. The inactivation of enveloped viruses appeared as the superior method to modify a fecal virome while maintaining its treatment efficacy against CDI, since FVT-SDT treated mice showed a survival rate of 8/8 mice, compared to 2/7, 5/7, and 5/8 mice for, respectively, the saline control, the non-modified fecal virome (FVT-UnT) and chemostat propagated virome (FVT-ChP). The systemic inflammatory response that occurs during CDI is driven by the *C. difficile* toxins that increase gut tissue permeability *(27, 28)* and thereby make the gut more susceptible to other microbial infections *(29, 30)*. Thus, a transfer of fecal donor viromes may lead to additional inflammation due to other microbes translocating through the damaged intestinal tissue. The mild symptoms and high survival rate associated with the FVT-SDT-treated mice could be explained by the loss of the lipid membrane of enveloped viruses in the fecal virome, thereby causing less inflammation. This may be in line with enveloped viruses belonging to the family *Herpesviridae*, which represent several major mammal pathogens *(31)*, were detected in the FVT-SDT inoculum (Fig. 5). The inactivation of this viral family might have contributed to the safety and efficacy associated with the FVT-SDT treatment compared to the untreated equivalent of FVT-UnT. It should be emphasized that the inactivation by dissolving the viral envelope does not exclude detecting the viruses by sequencing.

FMT is generally associated with more than 90% treatment efficacy in preclinical *(32, 33)* and clinical CDI studies *(3)*. Surprisingly, the FMT treated mice had a similar survival rate as the saline solution (control). The 16S rRNA gene analysis showed that the FMT inoculum contained ~ 20% relative abundance of the *Clostridium sensu stricto* spp., which has been associated to *C. difficile* positive calves *(34)* and to diarrhea in pigs *(35)*. The relatively high abundance of *Clostridium sensu stricto* spp. in the FMT inoculum may have counteracted the curing effect associated with FMT *(3, 32, 33)*. Although the FMT and FVT inoculum originated from the same donor material, the bacterial component is removed when processing the FVT. This could explain the higher survival rate associated with FVT-UnT, -ChP, and -SDT compared to FMT. This also suggests that even unsuitable fecal donor material for FMT could potentially be applicable for FVT. The lowest survival rate was associated with the RNA-targeting compound pyronin Y (FVT-PyT), where only 1/8 of the mice survived. In the initial evaluation of pyronin Y's abilities to inactivate RNA phages,

it was clear that also DNA phages were affected (Fig. 1). Thus, the pyronin Y treatment may have caused a reduction in phage activity that affected the potency of the treatment, which also would be in line with other studies that point to phages as a driving factor in restoring the GM balance after FMT or FVT *(3, 8–10, 15, 36–38)*.

A recent study has shown that *C. difficile* senses the mucus layer since it chemotax toward mucin and the glycan components. It was also reported that mucin-degrading bacteria like *Akkermansia muciniphila*, *Bacteroides thetaiotaomicron*, and *Ruminococcus torque* allow *C. difficile* to grow together in culture media containing purified MUC2, despite that *C. difficile* lacks the glycosyl hydrolases needed for degrading mucin glycans *(39)*. Co-existence of these bacterial taxa may explain why the euthanized mice tended to lose most of the commensal bacteria like *Prevotella* spp., *Lactobacillus* spp., *Turibacter* spp., *Bifidobacterium* spp., while *Akkermansia* and *Bacteroidetes* spp. persisted. Preventive use of frequent administration of high doses of *A. muciniphila* has been shown to alleviate CDI-associated symptoms in a similar mouse model *(40)*, which points in the direction of a co-existence rather than a symbiosis between *C. difficile* and mucin-degrading bacteria.

The different FVT treatment's ability to limit the abundance of the infectious *C. difficile* strain (Fig. 3A-3C) was linked with the survival rate, histology, and cytokine profiles. This was emphasized by ~1.5 – 2.0 $\log_{10}$ decrease in *C. difficile* abundance in mice treated with FVT-UnT, -ChP, and -SDT compared to saline, FMT, and FVT-PyT. Hence, if less *C. difficile* cells are present to produce the CDI etiology associated toxins *(27, 28)*, less cells will reach the stationary growth phase where the toxin production is the highest *(41)*. We believe that the phages transferred along with the FVT represent phages that allow commensal bacteria (that are associated with a healthy state) to compete with the infectious *C. difficile* strain as well as commensal bacteria that under certain conditions can act as a pathogen. This could be supported by a significant ($p < 0.05$) increase in the relative abundance of viruses that was predicted to infect *Escherichia*/*Shigella*, *Parabacteroides*, and *Bacteroides*, while these same bacterial genera had a significant decrease ($p < 0.05$) in the bacterial relative abundance when comparing the survived mice with the euthanized mice. There was no evidence of specific *C. difficile* phages, although it cannot be excluded. The suggested phage-mediated regulation of the GM was also supported by the bacterial and viral composition and diversity of the surviving mice that were pushed in the direction of the initial baseline GM profile (Fig. 4 and 5).

Instead of several termination points for all groups, only 8 mice per group were used in this study design to comply with the 3Rs principles (replacement, reduction, and refinement *(42)*). However, the natural consequences of euthanizing animals that reached the humane endpoint at different time points limited the statistical power of each group. Furthermore, it was not possible to sample feces at all time points for all mice. Despite these challenges, clear and statistically significant differences in phenotypical parameters could be observed, emphasizing the model's robustness. The metavirome sequencing of the feces samples only revealed ssRNA viruses (phages) belonging to the family *Leviviridae*, while the positive controls of both the dsRNA Phi6 and ssRNA MS2 phages (titer ~10^6 PFU/mL) were detected in both mock communities and spiked fecal samples (Fig. S9), suggesting that the metavirome library preparation was able to detect RNA viruses at concentrations at least above ~10^6 viral particles/mL. The sparse detection of enteric RNA viruses in our study may be due to insufficient viral databases *(43)*, that specific pathogen-free (SPF) mice are "too clean" *(44, 45)*, or that the concentration of these viruses was below the detection limit (~10^6 viral particles/mL) of both library preparation and/or sequencing depth.

A major challenge of CDI is the risk of recurrent infections *(46–48)*. Interestingly, the potential depletion of *C. difficile* in 7 out of 8 FVT-SDT-treated mice at termination highlights the possibility of decreasing the risks of recurrent infections with this modified virome. Treating fecal viromes with solvent-detergent prior to transfer to a patient may be especially relevant for gut-associated diseases, due to the increased gut tissue permeability *(29, 30)*. Despite the solvent-detergent treatment of the fecal virome (FVT-SDT) was superior to the other treatments against CDI in our study, the treatment efficacy and decrease in CDI-associated symptoms remained promising for the chemostat propagated virome (FVT-ChP). When optimized, this approach has the potential for higher reproducibility, standardization, large-scale production, increased removal of eukaryotic viruses by further dilution, and depends on only a few effective donors. It could therefore be argued that the solvent-detergent methodology, which already is approved by WHO for treating blood prior to transfusions *(49)*, harbors the potential for supplementing FMT in treating CDI in the short-term perspective. While a standardized and reproducible chemostat propagated phageome for CDI treatment may harbor a huge potential in the long-term perspectives.

METHODS

Detailed method descriptions can be found in the Supplementary Methods.

Study design - *Clostridioides difficile* infection model

The *C. difficile* infection model was based on Chen et al. 2008 *(26)*. Forty-eight female C57BL/6J (JAX) mice at the age of 8 weeks were purchased from Charles River Laboratories (European distributor of JAX mice) and subsequently housed at the animal facilities of Department of Experimental Medicine (AEM, University of Copenhagen, Denmark) in Innovive disposable IVC cages containing water, food (chow diet, Altromin 1324), bedding, cardboard housing, nesting material, felt pad, and biting stem. Mice were ear tagged upon arrival, housed 4 mice per cage, and then acclimatized for one week (Fig. 6). An antibiotic mixture (kanamycin 0.4 mg/mL, gentamicin 0.035 mg/mL, colistin 850 U/mL, metronidazole 0.215 mg/mL, and vancomycin 0.045 mg/mL) was prepared in the drinking water and mounted to the IVCs for 3 days, whereafter it was replaced with clean antibiotic-free drinking water for 2 days. The mice were then injected intraperitoneally with clindamycin 2 mg/mL that was diluted in sterile 0.9% (w/v) NaCl water (based on the average weight of the mice around 20 g) and followed by inoculation of 1.21 x 10^4 CFU of *C. difficile* VPI 10463 (CCUG 19126) by oral gavage 24 hours later. The mice were then divided into six different groups (n = 8) according to the different treatments: Saline (control), FMT, FVT-UnT (untreated FVT), FVT-ChP (chemostat propagated donor virome), FVT-SDT (solvent/detergent treated FVT for inactivating enveloped viruses), FVT-PyT (FVT treated with pyronin Y for inactivation of RNA viruses), and received 0.15 mL of the respective treatments twice by oral gave 18 hours and 72 hours after *C. difficile* inoculation (Fig. 6). Unfortunately, one mouse from the saline-treated group was euthanized immediately after oral gavage of *C. difficile* as the culture was accidentally administered via the trachea, which reduced this group to n = 7. One mouse from the FVT-UnT group was also euthanized due to malocclusions that had led to malnutrition which also reduced this group to n = 7. Frequent (up to every 3rd hour – day and night) monitoring of the animal health status was performed after *C. difficile* infection to evaluate if the mice had reached the humane endpoint, and if so, it led to immediate euthanization. The monitoring was supervised by the veterinarian associated with the study (AVM). The following qualitative parameters were used: the level of physical activity (e.i. decreased spontaneous or provoked activity), level of watery feces, body posture (hunching), and whether their fur was kept clean or not. The animals were scored from 0-2: The score of 0 (healthy), 1 (mild symptoms), 2 (clear symptoms). Mice with score

2 that showed no improvements in the above parameters within the next checkup were euthanized. Feces pellets were sampled (when possible) at different time points until termination of the mice (Fig. 6). At euthanization, the intestinal content from the cecum and colon was sampled, and a part of the cecum tissue *(50)* was fixated in 10% neutral-buffered formalin (Sarstedt) for histological analysis and stored at room temperature, and another part of the cecum tissue was preserved for cytokine analysis and stored at -80°C along with the intestinal content. All procedures regarding the handling of these animals were carried out in accordance with the Directive 2010/63/EU and the Danish Animal Experimentation Act with the license ID: 2021-15-0201-00836.

Preparation of the *Clostridioides difficile* inoculum

Clostridioides difficile VPI 10463 (CCUG 19126), originating from a human infection, was used as infectious agent in the mouse CDI described by Chen et al. *(26)*. The bacteria were cultured in brain-heart-infusion supplement (BHIS) medium *(51)* with 0.02% (w/v) 1,4-dithiothreitol (Fisher Scientific) and 0.05% (w/v) L-cysteine (Fisher Scientific), grown at 37°C in Hungate tubes (SciQuip), and handled anaerobically as previously described *(52)*. The cell concentration of the CDI inoculum was evaluated with CFU counts on BHIS agar plates (Fig. S10).

Propagation of host-phage pairs

The bacteria were grown in media and at a temperature suitable for each strain (Table S2). Five different bacteriophages (phages), along with their bacterial hosts, were included to assess the influence of pyronin Y and solvent/detergent treatment on RNA and DNA phage activity; *Lactococcus* phage c2 (host *Lactococcus lactic* MG1363), coliphage T4 (*Escherichia coli* Luria), coliphage phiX174 (*E. coli* PC 0886), coliphage MS2, (*E. coli* W1485), and *Pseudomonas* phage phi6 (*Pseudomonas* sp. HER1102).

The animal origin and preparation of donor viromes and FMT

In total 54 C57BL/6N male mice were purchased to harvest intestinal content for downstream applications. The mice were five weeks old at arrival and purchased from three vendors, represented by 18 C57BL/6NTac mice (Taconic, Denmark), 18 C57BL/6NRj mice (Janvier, France), and 18 C57BL/6NCrl mice (Charles River, Germany) and earmarked at arrival. Animal housing was carried out at Section of Experimental Animal Models, University of Copenhagen, Denmark, under conditions as described previously *(53)*. For 13 weeks the mice were fed ad libitum low-fat diet (LF, Research Diets D12450J) until termination as 18 weeks old. Malocclusions had led to malnutrition in two C57BL/6NRj mice which therefore were euthanized before planned

termination. All mice were sacrificed by cervical dislocation, and intestinal content from the cecum and colon was sampled and suspended in 500 µL autoclaved anoxic PBS buffer (NaCl 137 mM, KCl 2.7 mM, Na2HPO4 10 mM, KH2PO4 1.8 mM). All samples were subsequently stored at −80°C. To preserve the strict anaerobic bacteria, 6 mice from each vendor (in total 18 mice) were sacrificed and immediately transferred to an anaerobic chamber (containing ~93 % N_2, ~2 % H_2, ~5 % CO_2 and an atmosphere kept at room temperature, Coy Laboratory) for anoxic sampling of intestinal content that was used for subsequent fecal microbiota transplantation (FMT) and for anaerobic chemostat cultivation to produce the FVT-ChP. The intestinal content from the remaining 34 mice was sampled in aerobic atmosphere and were used to generate the fecal virome for downstream applications of the FVT-UnT, FVT-SDT, and FVT-PyT treatments. The abovementioned processes are illustrated with a flow-diagram (Fig. S11). All procedures for handling of animals used for donor material were carried out in accordance with the Directive 2010/63/EU and the Danish Animal Experimentation Act with the license ID: 2012-15-2934-00256.

Untreated fecal virome (FVT-UnT)

Intestinal content from cecum and colon was thawed and processed to produce FVT solutions as previously described *(9)*, with the exception of using Centriprep Ultracel YM-30K units (Millipore) instead of YM-50K units for concentrating filtrates and removing metabolites below the size of 30 kDa. The fecal viromes were mixed according to cages (due to their coprophagic behavior *(54, 55)*) to ensure the possibility to trace back the origin of specific bacterial or viral taxa. These fecal viromes were mixed into one mixture from mice of all three vendors representing the "untreated fecal virome", FVT-UnT, which was immediately stored at -80°C. The remaining fecal viromes were stored at 4°C prior to downstream processing to inactivate the eukaryotic viruses in the fecal viromes by either dissolving the lipid membrane of enveloped viruses with solvent/detergent (S/D) treatment or inhibit replication of RNA viruses with pyronin Y treatment.

Solvent/detergent treated fecal virome (FVT-SDT)

The solvent/detergent (S/D) treatment is commonly used for inactivating enveloped viruses (most eukaryotic viruses are enveloped) in blood plasma, while non-enveloped viruses (most phages are non-enveloped) are not inactivated *(56–58)*. The fecal viromes were treated by following the recommendations from the World Health Organization (WHO) for clinical use of S/D treated plasma; incubation in 1% (w/v) tri(n-butyl) phosphate (TnBP) and 1% (w/v) Triton X-100 at 30°C

for 4 hours *(49)*. Most inactivation usually occurs within the first 30-60 minutes of the S/D treatment *(49)*. S/D treatment was performed by following the method of Horowitz *et al.* *(56)* and the removal of TnBP and Triton X-100 were performed as described by Treščec *et al.* *(59)*. The removal of the S/D agents from the fecal viromes yielded approx. 100 mL viral-flow-through from the column which was concentrated to 0.5 mL using Centriprep Ultracel YM-30K units as described in the previous section. The final product constituted the FVT-SDT treatment. The effect of the S/D treatment on phage activity was assessed with traditional plaque assay of both non-enveloped phages (C2, T4, and phiX174) and one enveloped phage (phi6).

Pyronin Y treated fecal virome (FVT-PYT)

Pyronin Y (Merck) is a fluorescent compound (strong, red-colored dye) that has been reported to efficiently bind to ss/dsRNA, while the binding to ss/dsDNA is less efficient *(60, 61)*. Initial screening to determine optimal conditions of inactivation with different pyronin Y concentrations, incubation time, and temperature of different RNA and DNA phages was performed. Fecal filtrate was treated with 100 µM pyronin Y and incubated at 40°C overnight to inactivate viral particles containing RNA genomes. The non-bound pyronin Y molecules were removed by diluting the pyronin y treated fecal filtrate suspensions in 50 mL SM-buffer followed by concentration to 0.5 mL with Centriprep Ultracel YM-30K units. This process was repeated three times and resulted in an almost transparent appearance of the pyronin Y-treated fecal filtrate, which constituted the FVT-PyT treatment.

Fecal microbiota transplantation (FMT)

The mouse intestinal content that was sampled anaerobically (Fig. S11) was diluted 1:20 in an anoxic cryoprotectant consisting of PBS buffer and 20% (v/v) glycerol and stored at -80°C until administration.

Chemostat propagated fecal virome (FVT-ChP)

The preparation of the chemostat propagated virome was performed as described previously *(25)*. In brief, anaerobic-handled mouse cecum content was used for chemostat propagation. The culture medium was designed to mimic the LF diet (Research Diets D12450J) that the donor mice were provided as feed (Table S3), and the growth conditions as temperature, pH, etc. were set to mimic the environmental conditions found in mouse cecum. The end cultures fermented with a slow dilution rate (0.05 volumes 1/h) showed to generate a microbial composition closest to the donor's

initial microbial composition profile *(25)*, and these batches were mixed and constituted the applied FVT-ChP treatment.

Fluorescence microscopy

Virus-like particle (VLP) counts were evaluated of the fecal viromes (FVT-UnT, FVT-SDT, FVT-ChP, and FVT-PyT, Fig. S12) by epifluorescence microscopy using SYBR Gold staining (Thermo Scientific) as described online dx.doi.org/10.17504/protocols.io.bx6cpraw.

Cytokine analysis

Pre-weighted cecum tissue was homogenized in 400µl lysis buffer (stock solution: 10ml Tris lysis buffer, 100µl phosphatase inhibitor 1, 100µl phosphatase inhibitor 2, and 200µl protease inhibitor (MSD inhibitor pack, Mesoscale Discovery, Rockville, MD) using a tissue blender (POLYTRON PT 1200 E, Kinematica, Luzern, Switzerland), and centrifuged (7,500g; 4°C; 5 min). Samples were diluted 1:2 and analyzed for IFN-γ, IL-1β, IL-2, IL-4, IL-5, IL-6, IL-10, IL-12p70, KC/GRO, and TNF-α with V-PLEX Proinflammatory Panel 1 Mouse kit (Mesocale Discovery) and for MIP-3α, IL-16, IL-17A, IL-17C, IL-17E, IL-17F, IL-21, IL-22, IL-23, and IL-31 with V-PLEX Th17 Panel 1 Mouse (Mesoscale Discovery) according to manufacturer's instructions. Measurements out of detection range (missing values) were assigned the lower or upper detection limit value. Concentrations were extrapolated from a standard curve using Mesoscale's own Discovery Workbench analysis software and normalized to total protein measured with Pierce Detergent Compatible Bradford Assay kit according to manufacturer's protocol.

Histology and cytotoxicity assay

Formalin-fixed, paraffin-embedded cecum tissue sections were stained with hematoxylin and eosin for histopathological evaluation by a blinded investigator. A composite score was assigned, taking into account the following pathological features: 1) immune cell infiltration, 2) submucosal edema or hemorrhage, 3) epithelial injury, each with a range of severity/extent as follows: 0: none, 1: mild, 2: moderate, 3: severe) for a cumulative pathology grade between 0 and 9 *(9)*. The RIDASCREEN *Clostridium difficile* Toxin A/B ELISA kit (r-biopharm) was used to measure the toxin concentrations in the mice feces by following the instructions of the manufacturer. The OD_{450nm} was measured with a Varioskan Flash plate reader (Thermo Fisher Scientific).

Quantitative real-time PCR measuring *C. difficile* abundance

C. difficile in the fecal samples was enumerated using quantitative real-time polymerase chain reaction (qPCR) with specie specific primers (C.Diff_ToxA_Fwd: 5'-TCT ACC ACT GAA GCA

TTA C-3', C.Diff_ToxA_Rev: 5'-TAG GTA CTG TAG GTT TAT TG-3' *(62)*) purchased from Integrated DNA Technologies. Standard curves (Table S4) were based on a dilution series of total DNA extracted from monocultures *C. difficile* VPI 10463. The qPCR results were obtained using the CFX96 Touch Real-Time PCR Detections System (Bio-Rad Laboratories) and the reagent RealQ plus 2x Master Mix Green low Rox (Amplicon) as previously described *(63)*.

Pre-processing of fecal samples for separation of viruses and bacteria

Fecal samples from three different time points were included to investigate gut microbiome changes over time: baseline (before antibiotic treatment), before *C. difficile* infection, and at termination. This represented in total 144 fecal samples. Separation of the viruses and bacteria from the fecal samples generated a fecal pellet and fecal supernatant by centrifugation and 0.45 µm filtering as described previously *(53)*, except the volume of fecal homogenate was adjusted to 5 mL using SM buffer.

Bacterial DNA extraction, sequencing and pre-processing of raw data

The DNeasy PowerSoil Pro Kit (Qiagen) was used to extract bacterial DNA from the fecal pellet by following the instructions of the manufacturer. The final purified DNA was stored at -80ºC and the DNA concentration was determined using Qubit HS Assay Kit (Invitrogen) on the Qubit 4 Fluorometric Quantification device (Invitrogen). The bacterial community composition was determined by Illumina NextSeq-based high-throughput sequencing (HTS) of the 16S rRNA gene V3-region, as previously described *(53)*. Quality control of reads, de-replicating, purging from chimeric reads and constructing zOTU was conducted with the UNOISE pipeline *(64)* and taxonomy assigned with Sintax *(65)* using the EZtaxon for 16S rRNA gene database *(66)*. Code describing this pipeline can be accessed in github.com/jcame/Fastq_2_zOTUtable. The average sequencing depth after quality control (Accession: PRJEB58777, available at ENA) for the fecal 16S rRNA gene amplicons was 60,719 reads (min. 11,961 reads and max. 198,197 reads).

Viral RNA/DNA extraction, sequencing and pre-processing of raw data

The sterile filtered fecal supernatant was concentrated using Centrisart centrifugal filters with a filter cut-off at 100 kDA (Sartorius) by centrifugation at 1,500 x g at 4ºC (dx.doi.org/10.17504/protocols.io.b2qaqdse). The viral DNA/RNA was extracted from the fecal supernatants using the Viral RNA mini kit (Qiagen) as previously described *(53)*. Reverse transcription was executed with SuperScript IV VILO Master mix by following the instructions of the manufacturer and subsequently cleaned with DNeasy blood and tissue kit (Qiagen) by only

following step 3-8 in the instructions from the manufacturer. In brief, the DNA/cDNA samples were mixed with ethanol, bound to the silica filter, washed two times, and eluted with 40 µL elution buffer. Multiple displacement amplification (MDA, to include ssDNA viruses) using GenomiPhi V3 DNA amplification kit (Cytiva) and sequencing library preparation using the Nextera XT kit (Illumina) was performed at previously described *(53)*, and sequenced using the Illumina NovaSeq platform at the sequencing provider Novogene (Cambridge, UK). The average sequencing depth of raw reads (Accession: PRJEB58777, available at ENA) for the fecal viral metagenome was 17,384,372 reads (min. 53,960 reads and max. 81,642,750 reads. Pre-processing of raw sequencing data and viral contig assembly were performed as previously described *(11)*. Code describing this pipeline can be accessed in github.com/jcame/virome_analysis-FOOD.

Bioinformatic analysis of bacterial and viral sequences

Initially the dataset was purged for zOTU's/viral contigs, which were detected in less than 5% of the samples, but the resulting dataset still maintained >99.8% of the total reads. Cumulative sum scaling (CSS) *(67)* was applied for the analysis of beta-diversity. CSS normalization was performed using the R software using the metagenomeSeq package *(68)*. R version 4.2.2 *(69)* was used for subsequent analysis and presentation of data. The main packages used were phyloseq *(70)*, vegan *(71)*, deseseq 2 *(72)*, ampvis2 *(73)*, ggpubr *(74)* and ggplot2 *(74)*.

Statistical analysis

Alpha-diversity analysis was based on raw read counts and statistics were based on ANOVA. Beta-diversity was represented by Bray Curtis dissimilarity and statistics were based on PERMANOVA. T-test with pooled standard deviations was applied to assess the statistically differences between the treatment groups of cytokine levels, toxin levels, *C. difficile* abundance, and histology, while log rank test was used to compare the survival distributions.

List of Supplementary Materials

This PDF file includes:

Supplementary Methods

Fig. S1 to S12

Table S1 to S4

Acknowledgement

We thank the staff of veterinarians and animal caretakers at the Department of Experimental Medicine (AEM, University of Copenhagen, Denmark) for their cooperation of housing, handling,

and monitoring of the mice. Also, a thank you to PhD Casper Normann Nurup, who assisted in the initial setup of the column chromatography, and lab trainee Mariam Al-Batool Samir S Bagi, who performed the ELISA assay. Last, a thanks to the Food & Health Open Innovation project (FOODHAY) granted by the Danish Ministry of Education and Research for funding the qPCR equipment (Bio-Rad Laboratories CFX96) applied in this study.

Funding

Funding was provided by:

The Lundbeck Foundation with grant ID: R324-2019-1880 under the acronym “SafeVir”.

The Novo Nordisk Foundation with grant ID: NNF-20OC0063874 under the acronym “PrePhage”.

Author contributions

Conceptualization: TSR, DSN

Methodology: TSR, SF, SBL, KDT, AVM (veterinarian, supervising the health status monitoring), AB, JLCM, SA, KA, CHFH

Investigation: TSR, SF, AB, AVM, CHFH, AKH, DSN

Visualization: TSR, AB

Funding acquisition: TSR, DSN

Project administration: TSR, DSN

Supervision: DSN, AKH

Writing – original draft: TSR

Writing – review & editing: All authors critically revised and approved the final version of the manuscript.

Competing interests

All authors declare no conflicts of interest.

Data and materials availability

All data associated with this study are present in the paper or the Supplementary Materials. All sequencing datasets are available in the ENA database under accession number PRJEB58777.

References

1. B. Millan, H. Park, N. Hotte, O. Mathieu, P. Burguiere, T. A. Tompkins, D. Kao, K. L. Madsen, Fecal Microbial Transplants Reduce Antibiotic-resistant Genes in Patients With Recurrent Clostridium difficile Infection. *Clin Infect Dis* **62**, 1479–1486 (2016).
2. P. Maruvada, V. Leone, L. M. Kaplan, E. B. Chang, The Human Microbiome and Obesity: Moving beyond Associations. *Cell Host Microbe* **22**, 589–599 (2017).
3. S. J. Ott, G. H. Waetzig, A. Rehman, J. Moltzau-Anderson, R. Bharti, J. A. Grasis, L. Cassidy, A. Tholey, H. Fickenscher, D. Seegert, P. Rosenstiel, S. Schreiber, Efficacy of Sterile Fecal Filtrate Transfer for Treating Patients With Clostridium difficile Infection. *Gastroenterology* **152**, 799-811.e7 (2017).
4. S. Gupta, E. Allen-Vercoe, E. O. Petrof, Fecal microbiota transplantation: in perspective. *Therap Adv Gastroenterol* **9**, 229–39 (2016).
5. FDA, Important safety alert regarding use of FMT (2019) (available at https://www.fda.gov/vaccines-blood-biologics/safety-availability-biologics/important-safety-alert-regarding-use-fecal-microbiota-transplantation-and-risk-serious-adverse).
6. D. H. Kao, B. Roach, J. Walter, R. Lobenberg, K. Wong, Effect of lyophilized sterile fecal filtrate vs lyophilized donor stool on recurrent Clostridium difficile infection (rCDI): Prelimenary results from a randomized, double-blind pilot study. *J Can Assoc Gastroenterol* **2**, 101–102 (2019).
7. Z. Cao, N. Sugimura, E. Burgermeister, M. P. Ebert, T. Zuo, P. Lan, The gut virome: A new microbiome component in health and disease. *EBioMedicine* **81**, 104113 (2022).
8. L. A. Draper, F. J. Ryan, M. Dalmasso, P. G. Casey, A. McCann, V. Velayudhan, R. P. Ross, C. Hill, Autochthonous faecal viral transfer (FVT) impacts the murine microbiome after antibiotic perturbation. *BMC Biol* **18**, 173 (2020).
9. T. S. Rasmussen, C. M. J. Mentzel, W. Kot, J. L. Castro-Mejía, S. Zuffa, J. R. Swann, L. H. Hansen, F. K. Vogensen, A. K. Hansen, D. S. Nielsen, Faecal virome transplantation decreases symptoms of type 2 diabetes and obesity in a murine model. *Gut* **69**, 2122–2130 (2020).
10. A. Brunse, L. Deng, X. Pan, Y. Hui, J. L. Castro-Mejía, W. Kot, D. N. Nguyen, J. B.-M. Secher, D. S. Nielsen, T. Thymann, Fecal filtrate transplantation protects against necrotizing enterocolitis. *ISME J* **16**, 686–694 (2022).
11. T. S. Rasmussen, C. M. J. Mentzel, M. Refslund, R. R. Jakobsen, L. S. F. Zachariassen, L. Castro-Mejia, L. H. Hansen, A. K. Hansen, D. S. Nielsen, Fecal virome transfer improves proliferation of commensal gut Akkermansia muciniphila and unexpectedly enhances the fertility rate in laboratory mice. *bioRxiv* (2022), doi:10.1101/2022.06.30.498243.
12. S. A. Shah, L. Deng, J. Thorsen, A. G. Pedersen, M. B. Dion, J. L. Castro-Mejía, R. Silins, F. O. Romme, R. Sausset, E. O. Ndela, M. Hjemlsø, M. A. Rasmussen, T. A. Redgwell, G. Vestergaard, Y. Zhang, S. J. Sørensen, H. Bisgaard, F. Enault, J. Stokholm, S. Moineau, M.-A. Petit, D. S. Nielsen, Hundreds of viral families in the healthy infant gut. *bioRxiv* (2022), doi:10.1101/2021.07.02.450849.
13. E. S. Lim, Y. Zhou, G. Zhao, I. K. Bauer, L. Droit, I. M. Ndao, B. B. Warner, P. I. Tarr, D. Wang, L. R. Holtz, Early life dynamics of the human gut virome and bacterial microbiome in infants. *Nat Med* **21**, 1228–1234 (2015).
14. J. Doorbar, N. Egawa, H. Griffin, C. Kranjec, I. Murakami, Human papillomavirus molecular biology and disease association. *Rev Med Virol* **25**, 2–23 (2015).
15. T. S. Rasmussen, A. K. Koefoed, R. R. Jakobsen, L. Deng, J. L. Castro-Mejía, A. Brunse, H. Neve, F. K. Vogensen, D. S. Nielsen, Bacteriophage-mediated manipulation of the gut microbiome - promises and presents limitations. *FEMS Microbiol Rev* **44**, 507–521 (2020).
16. F. D'Herelle, On an invisible microbe antagonistic toward dysenteric bacilli: brief note by Mr. F. D'Herelle, presented by Mr. Roux. 1917. *Res Microbiol* **158**, 553–4 (2007).
17. A. Górski, R. Miedzybrodzki, B. Weber-Dabrowska, W. Fortuna, S. Letkiewicz, P. Rogóz, E. Jończyk-Matysiak, K. Dabrowska, J. Majewska, J. Borysowski, Phage therapy: Combating infections with potential for evolving from merely a treatment for complications to targeting diseases. *Front Microbiol* **7**, 1–9 (2016).
18. R. K. Al-Ishaq, S. Skariah, D. Büsselberg, Bacteriophage Treatment: Critical Evaluation of Its Application on World Health Organization Priority Pathogens. *Viruses* **13** (2020), doi:10.3390/v13010051.
19. C. Loc-Carrillo, S. T. Abedon, Pros and cons of phage therapy. *Bacteriophage* **1**, 111–114 (2011).
20. D. Liu, J. D. van Belleghem, C. R. de Vries, E. Burgener, Q. Chen, R. Manasherob, J. R. Aronson, D. F. Amanatullah, P. D. Tamma, G. A. Suh, The Safety and Toxicity of Phage Therapy: A Review of Animal and Clinical Studies. *Viruses* **13**, 1–20 (2021).
21. F. A. Rey, S. M. Lok, Common Features of Enveloped Viruses and Implications for Immunogen Design for Next-Generation Vaccines*Cell* **172**, 1319–1334 (2018).

22. P. J. L. Bell, Evidence supporting a viral origin of the eukaryotic nucleus. *Virus Res* **289**, 198168 (2020).
23. E. v. Koonin, V. v. Dolja, M. Krupovic, Origins and evolution of viruses of eukaryotes: The ultimate modularity*Virology* **479–480**, 2–25 (2015).
24. R. Sausset, M. A. Petit, V. Gaboriau-Routhiau, M. De Paepe, New insights into intestinal phages. *Mucosal Immunol* **13**, 205–215 (2020).
25. S. Adamberg, T. S. Rasmussen, S. B. Larsen, D. S. Nielsen, K. Adamberg, Reproducible chemostat cultures to eliminate eukaryotic viruses from fecal transplant material. *bioRxiv* (2023), doi:10.1101/2023.03.15.529189.
26. X. Chen, K. Katchar, J. D. Goldsmith, N. Nanthakumar, A. Cheknis, D. N. Gerding, C. P. Kelly, A mouse model of Clostridium difficile-associated disease. *Gastroenterology* **135**, 1984–92 (2008).
27. R. Moore, C. Pothoulakis, J. T. LaMont, S. Carlson, J. L. Madara, C. difficile toxin A increases intestinal permeability and induces Cl- secretion. *Am J Physiol* **259**, G165-72 (1990).
28. K. Rao, J. R. Erb-Downward, S. T. Walk, D. Micic, N. Falkowski, K. Santhosh, J. A. Mogle, C. Ring, V. B. Young, G. B. Huffnagle, D. M. Aronoff, M. R. Popoff, Ed. The Systemic Inflammatory Response to Clostridium difficile Infection. *PLoS One* **9**, e92578 (2014).
29. S. C. Bischoff, G. Barbara, W. Buurman, T. Ockhuizen, J.-D. Schulzke, M. Serino, H. Tilg, A. Watson, J. M. Wells, Intestinal permeability - a new target for disease prevention and therapy. *BMC Gastroenterol* **14**, 189 (2014).
30. M. Camilleri, Leaky gut: mechanisms, measurement and clinical implications in humans. *Gut* **68**, 1516–1526 (2019).
31. V. Sharma, F. Mobeen, T. Prakash, Comparative Genomics of Herpesviridae Family to Look for Potential Signatures of Human Infecting Strains. *Int J Genomics* **2016**, 1–10 (2016).
32. Q. Xu, S. Zhang, J. Quan, Z. Wu, S. Gu, Y. Chen, B. Zheng, L. Lv, L. Li, The evaluation of fecal microbiota transplantation vs vancomycin in a Clostridioides difficile infection model. *Appl Microbiol Biotechnol* **106**, 6689–6700 (2022).
33. A. M. Seekatz, C. M. Theriot, C. T. Molloy, K. L. Wozniak, I. L. Bergin, V. B. Young, Fecal Microbiota Transplantation Eliminates Clostridium difficile in a Murine Model of Relapsing Disease. *Infect Immun* **83**, 3838–46 (2015).
34. L. E. Redding, A. S. Berry, N. Indugu, E. Huang, D. P. Beiting, D. Pitta, Gut microbiota features associated with Clostridioides difficile colonization in dairy calves. *PLoS One* **16**, e0251999 (2021).
35. J.-J. Zhu, M.-X. Gao, X.-J. Song, L. Zhao, Y.-W. Li, Z.-H. Hao, Changes in bacterial diversity and composition in the faeces and colon of weaned piglets after feeding fermented soybean meal. *J Med Microbiol* **67**, 1181–1190 (2018).
36. T. Zuo, S. H. Wong, K. Lam, R. Lui, K. Cheung, W. Tang, J. Y. L. Ching, P. K. S. Chan, M. C. W. Chan, J. C. Y. Wu, F. K. L. Chan, J. Yu, J. J. Y. Sung, S. C. Ng, Bacteriophage transfer during faecal microbiota transplantation in Clostridium difficile infection is associated with treatment outcome. *Gut* **67**, 634–643 (2018).
37. K. Fujimoto, Y. Kimura, J. R. Allegretti, M. Yamamoto, Y. Zhang, K. Katayama, G. Tremmel, Y. Kawaguchi, M. Shimohigoshi, T. Hayashi, M. Uematsu, K. Yamaguchi, Y. Furukawa, Y. Akiyama, R. Yamaguchi, S. E. Crowe, P. B. Ernst, S. Miyano, H. Kiyono, S. Imoto, S. Uematsu, Functional Restoration of Bacteriomes and Viromes by Fecal Microbiota Transplantation. *Gastroenterology* **160**, 2089-2102.e12 (2021).
38. X. Mao, S. B. Larsen, L. S. F. Zachariassen, A. Brunse, S. Adamberg, J. L. Castro-Meija, K. Adamberg, D. S. Nielsen, A. K. Hansen, C. H. F. Hansen, T. S. Rasmussen, A reproducible enteric phage community improves blood glucose regulation in an obesity mouse model. *bioRxiv* (2023), doi:10.1101/2023.03.20.532903.
39. M. A. Engevik, A. C. Engevik, K. A. Engevik, J. M. Auchtung, A. L. Chang-Graham, W. Ruan, R. A. Luna, J. M. Hyser, J. K. Spinler, J. Versalovic, Mucin-Degrading Microbes Release Monosaccharides That Chemoattract Clostridioides difficile and Facilitate Colonization of the Human Intestinal Mucus Layer. *ACS Infect Dis* **7**, 1126–1142 (2021).
40. Z. Wu, Q. Xu, S. Gu, Y. Chen, L. Lv, B. Zheng, Q. Wang, K. Wang, S. Wang, J. Xia, L. Yang, X. Bian, X. Jiang, L. Zheng, L. Li, Akkermansia muciniphila Ameliorates Clostridioides difficile Infection in Mice by Modulating the Intestinal Microbiome and Metabolites. *Front Microbiol* **13**, 841920 (2022).
41. C. Darkoh, H. L. DuPont, S. J. Norris, H. B. Kaplan, Toxin synthesis by Clostridium difficile is regulated through quorum signaling. *mBio* **6**, e02569 (2015).
42. J. MacArthur Clark, The 3Rs in research: a contemporary approach to replacement, reduction and refinement. *Br J Nutr* **120**, S1–S7 (2018).
43. N. Goodacre, A. Aljanahi, S. Nandakumar, M. Mikailov, A. S. Khan, M. J. Imperiale, Ed. A Reference Viral Database (RVDB) To Enhance Bioinformatics Analysis of High-Throughput Sequencing for Novel Virus Detection. *mSphere* **3**, 1–18 (2018).

641 44. T. S. Rasmussen, R. R. Jakobsen, J. L. Castro-Mejía, W. Kot, A. R. Thomsen, F. K. Vogensen, D. S. Nielsen, A.
642 K. Hansen, Inter-vendor variance of enteric eukaryotic DNA viruses in specific pathogen free C57BL/6N mice. *Res*
643 *Vet Sci* **136**, 1–5 (2021).
644 45. E. J. Fay, K. M. Balla, S. N. Roach, F. K. Shepherd, D. S. Putri, T. D. Wiggen, S. A. Goldstein, M. J. Pierson,
645 M. T. Ferris, C. E. Thefaine, A. Tucker, M. Salnikov, V. Cortez, S. R. Compton, S. v Kotenko, R. C. Hunter, D.
646 Masopust, N. C. Elde, R. A. Langlois, Natural rodent model of viral transmission reveals biological features of virus
647 population dynamics. *J Exp Med* **219** (2022), doi:10.1084/jem.20211220.
648 46. B. H. Mullish, M. N. Quraishi, J. P. Segal, V. L. McCune, M. Baxter, G. L. Marsden, D. J. Moore, A. Colville,
649 N. Bhala, T. H. Iqbal, C. Settle, G. Kontkowski, A. L. Hart, P. M. Hawkey, S. D. Goldenberg, H. R. T. Williams,
650 The use of faecal microbiota transplant as treatment for recurrent or refractory Clostridium difficile infection and
651 other potential indications: joint British Society of Gastroenterology (BSG) and Healthcare Infection Society (HIS)
652 guidelines. *Gut* **67**, 1920–1941 (2018).
653 47. W. Hui, T. Li, W. Liu, C. Zhou, F. Gao, Fecal microbiota transplantation for treatment of recurrent C. difficile
654 infection: An updated randomized controlled trial meta-analysis. *PLoS One* **14**, e0210016 (2019).
655 48. L. Martinez-Gili, J. A. K. K. McDonald, Z. Liu, D. Kao, J. R. Allegretti, T. M. Monaghan, G. F. Barker, J.
656 Miguéns Blanco, H. R. T. T. Williams, E. Holmes, M. R. Thursz, J. R. Marchesi, B. H. Mullish, Understanding the
657 mechanisms of efficacy of fecal microbiota transplant in treating recurrent Clostridioides difficile infection and
658 beyond: the contribution of gut microbial-derived metabolites. *Gut Microbes* **12**, 1810531 (2020).
659 49. WHO Health Product Policy and Standards Team, Guidelines on viral inactivation and removal procedures
660 intended to assure the viral safety of human blood plasma products, WHO-TRS924-Annex4-1-82 (2004).
661 50. E. R. Littmann, J.-J. Lee, J. E. Denny, Z. Alam, J. R. Maslanka, I. Zarin, R. Matsuda, R. A. Carter, B. Susac, M.
662 S. Saffern, B. Fett, L. M. Mattei, K. Bittinger, M. C. Abt, Host immunity modulates the efficacy of microbiota
663 transplantation for treatment of Clostridioides difficile infection. *Nat Commun* **12**, 755 (2021).
664 51. A. N. Edwards, S. M. McBride, A. P. Roberts, P. Mullany, Eds. Isolating and Purifying Clostridium difficile
665 Spores. *Methods Mol Biol* **1476**, 117–28 (2016).
666 52. T. S. Rasmussen, T. Streidl, T. C. A. Hitch, E. Wortmann, P. Deptula, M. V. W. Kofoed, T. Riedel, M.
667 Neumann-Schaal, M. Hansen, D. S. Nielsen, T. Clavel, F. K. Vogensen, Sporofaciens musculi gen. nov., sp. nov., a
668 novel bacterium isolated from the caecum of an obese mouse. *Int J Syst Evol Microbiol* **71** (2021),
669 doi:10.1099/ijsem.0.004673.
670 53. T. S. Rasmussen, L. de Vries, W. Kot, L. H. Hansen, J. L. Castro-Mejía, F. K. Vogensen, A. K. Hansen, D. S.
671 Nielsen, Mouse Vendor Influence on the Bacterial and Viral Gut Composition Exceeds the Effect of Diet. *Viruses*
672 **11** (2019), doi:10.3390/v11050435.
673 54. R. Bibiloni, Rodent models to study the relationships between mammals and their bacterial inhabitants. *Gut*
674 *Microbes* **3**, 536–543 (2012).
675 55. P. J. Torres, B. S. Ho, P. Arroyo, L. Sau, A. Chen, S. T. Kelley, V. G. Thackray, Exposure to a Healthy Gut
676 Microbiome Protects Against Reproductive and Metabolic Dysregulation in a PCOS Mouse Model. *Endocrinology*
677 **160**, 1193–1204 (2019).
678 56. B. Horowitz, R. Bonomo, A. M. Prince, S. N. Chin, B. Brotman, R. W. Shulman, Solvent/detergent-treated
679 plasma: a virus-inactivated substitute for fresh frozen plasma. *Blood* **79**, 826–31 (1992).
680 57. A. M. Prince, B. Horowitz, B. Brotman, Sterilisation of hepatitis and HTLV-III viruses by exposure to tri(n-
681 butyl)phosphate and sodium cholate. *Lancet* **1**, 706–10 (1986).
682 58. M. M. Remy, M. Alfter, M.-N. Chiem, M. T. Barbani, O. B. Engler, F. Suter-Riniker, Effective chemical virus
683 inactivation of patient serum compatible with accurate serodiagnosis of infections. *Clin Microbiol Infect* **25**, 907.e7-
684 907.e12 (2019).
685 59. A. Trescec, M. Simić, K. Branović, B. Gebauer, B. Benko, Removal of detergent and solvent from solvent-
686 detergent-treated immunoglobulins. *J Chromatogr A* **852**, 87–91 (1999).
687 60. Z. Darzynkiewicz, J. Kapuscinski, S. P. Carter, F. A. Schmid, M. R. Melamed, Cytostatic and cytotoxic
688 properties of pyronin Y: relation to mitochondrial localization of the dye and its interaction with RNA. *Cancer Res*
689 **46**, 5760–6 (1986).
690 61. J. Kapuscinski, Z. Darzynkiewicz, Interactions of pyronin Y(G) with nucleic acids. *Cytometry* **8**, 129–37 (1987).
691 62. S. Gillers, C. D. Atkinson, A. C. Bartoo, M. Mahalanabis, M. O. Boylan, J. H. Schwartz, C. Klapperich, S. K.
692 Singh, Microscale sample preparation for PCR of C. difficile infected stool. *J Microbiol Methods* **78**, 203–7 (2009).
693 63. M. Ellekilde, L. Krych, C. H. F. Hansen, M. R. Hufeldt, K. Dahl, L. H. Hansen, S. J. Sørensen, F. K. Vogensen,
694 D. S. Nielsen, A. K. Hansen, Characterization of the gut microbiota in leptin deficient obese mice - Correlation to
695 inflammatory and diabetic parameters. *Res Vet Sci* **96**, 241–50 (2014).

64. R. C. Edgar, A. Valencia, Ed. Updating the 97% identity threshold for 16S ribosomal RNA OTUs. *Bioinformatics* **34**, 2371–2375 (2018).
65. R. Edgar, SINTAX: a simple non-Bayesian taxonomy classifier for 16S and ITS sequences. *bioRxiv* , 074161 (2016).
66. O.-S. Kim, Y.-J. Cho, K. Lee, S.-H. Yoon, M. Kim, H. Na, S.-C. Park, Y. S. Jeon, J.-H. Lee, H. Yi, S. Won, J. Chun, Introducing EzTaxon-e: a prokaryotic 16S rRNA gene sequence database with phylotypes that represent uncultured species. *Int J Syst Evol Microbiol* **62**, 716–721 (2012).
67. J. N. Paulson, O. C. Stine, H. C. Bravo, M. Pop, Differential abundance analysis for microbial marker-gene surveys. *Nat Methods* **10**, 1200–2 (2013).
68. J. Paulson, metagenomeSeq: Statistical analysis for sparse high-throughput sequencing. *Bioconductor.Jp* , 1–20 (2014).
69. R. C. Team, R: A language and environment for statistical title.
70. P. J. McMurdie, S. Holmes, M. Watson, Ed. phyloseq: an R package for reproducible interactive analysis and graphics of microbiome census data. *PLoS One* **8**, e61217 (2013).
71. P. Dixon, VEGAN, a package of R functions for community ecology. *Journal of Vegetation Science* **14**, 927–930 (2003).
72. M. I. Love, W. Huber, S. Anders, Moderated estimation of fold change and dispersion for RNA-seq data with DESeq2. *Genome Biol* **15**, 550 (2014).
73. K. S. Andersen, R. H. Kirkegaard, S. M. Karst, M. Albertsen, ampvis2: an R package to analyse and visualise 16S rRNA amplicon data. *bioRxiv* (2018), doi:10.1101/299537.
74. H. Wickham, ggplot2. *Wiley Interdiscip Rev Comput Stat* **3**, 180–185 (2011).

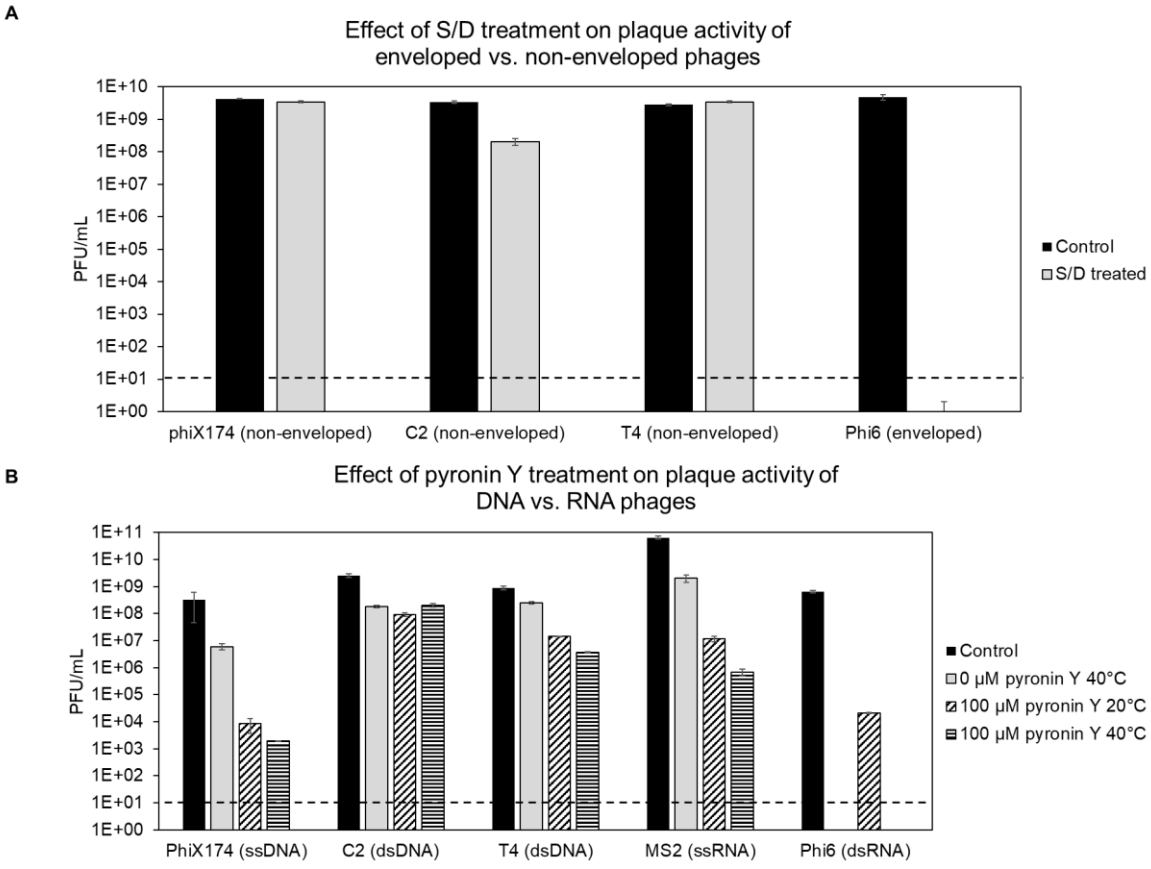

Fig. 1: Evaluation of inactivation of phage activity with solvent/detergent or pyronin Y treatment. A) Three enveloped phages (phiX174, C2, and T4) and one enveloped phage (phi6) were treated with solvent/detergent and their plaque activity (plaque forming units per mL) was evaluated on their respective bacterial hosts. B) Phages representing ssDNA (phiX174), dsDNA (C2 and T4), ssRNA (MS2), and dsRNA (phi6) were treated with pyronin Y and their plaque activity (PFU/mL) at different incubation conditions was evaluated on their respective bacterial hosts. Dashed lines mark the detection limit of the applied assay.

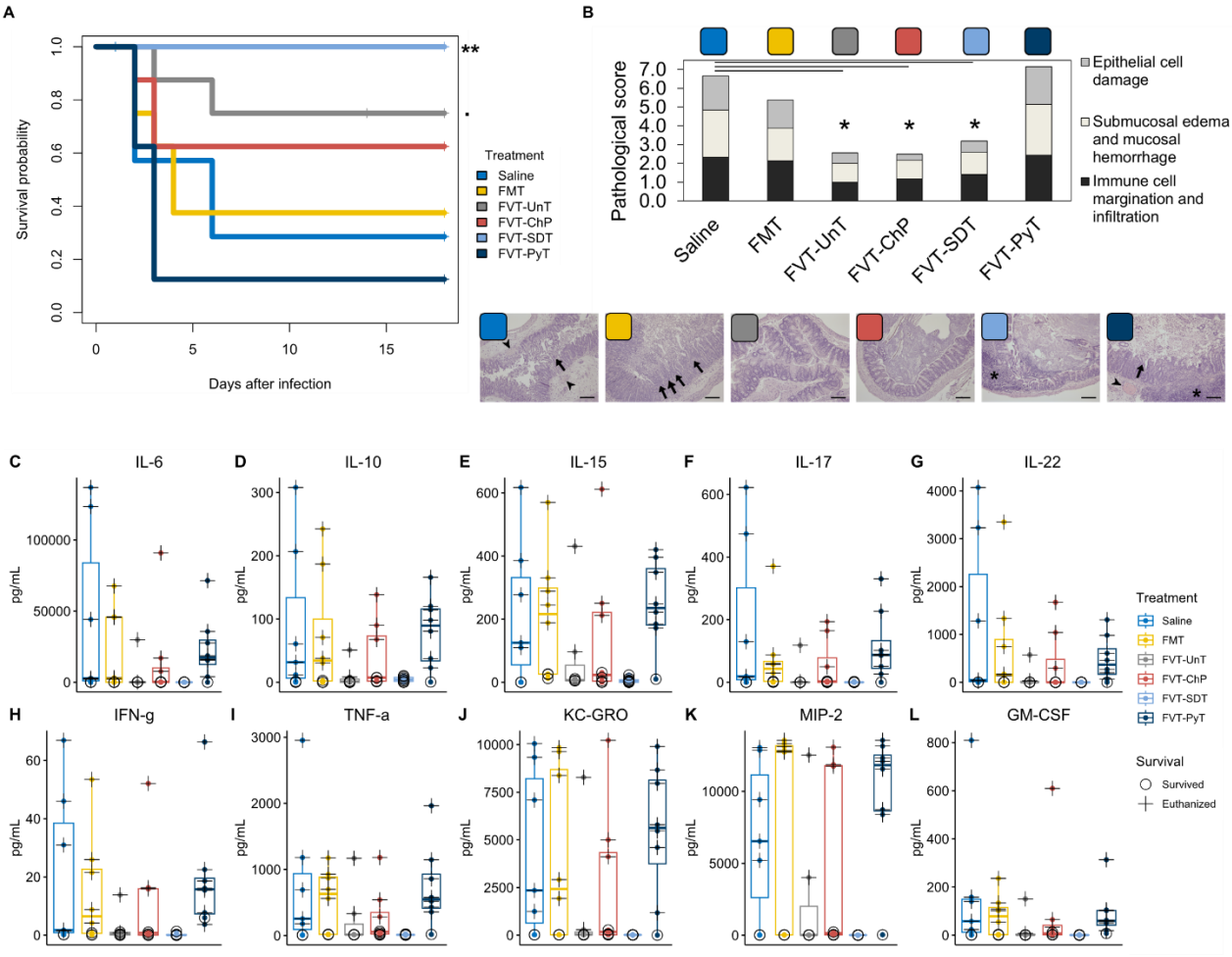

Fig. 2: Overview of mouse phenotypic characteristics. A) Kaplan-Meier curve showing the survival probability of the mice that was associated to the different treatments. B) Pathological score and representative histology images of cecum tissue evaluating the effect of the treatments' ability to prevent *C. difficile* associated damage of the cecum tissue. C) to L) Showing the overall cytokine profile in the mouse cecum tissue of the different treatments. The euthanized (cross) mice are differentiated from the mice that survived (circle) the *C. difficile* infection. "**" = $p < 0.005$, "*" = $p < 0.05$, "." = $p < 0.1$. Histology image scale = 300 µm, Asterisks = immune cell infiltrates, arrowheads = congested submucosal blood vessels, arrows = volcano lesions contributing to pseudo-membrane formation.

735

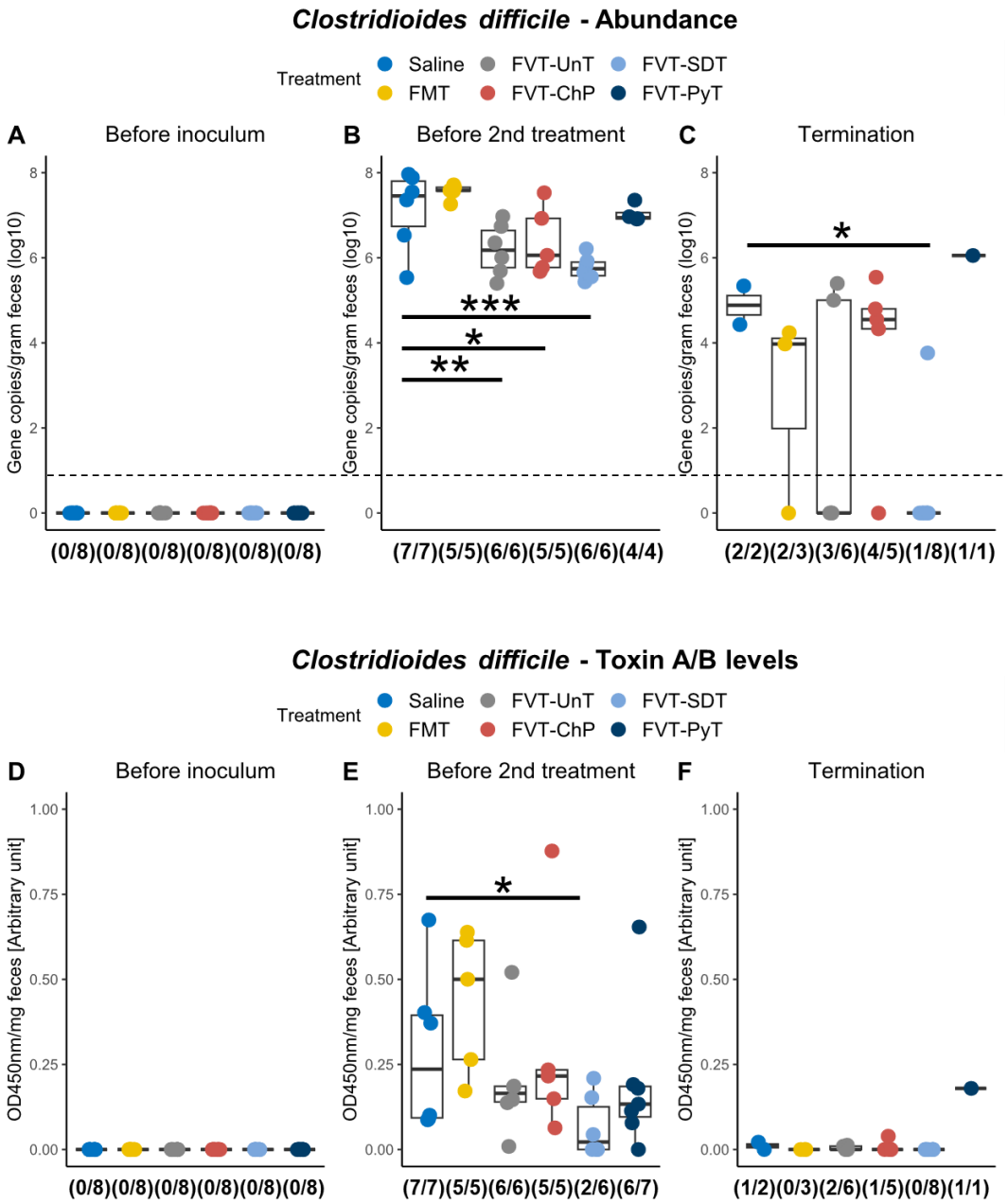

736

737 Fig. 3: Evaluation of *C. difficile* abundance A) to C) by qPCR targeting the toxA gene and D) to F) the associated toxin A/B levels
738 measured with ELISA on feces samples from three different time points: before *C. difficile* inoculum, before 2nd treatment, and at
739 study termination. The fraction below the bar plots highlights the number of mice that were detected positive of either *C. difficile*
740 or toxin A/B. Dashed line marks the detection limit of the applied assay. * = $p < 0.05$, ** = $p < 0.01$, *** = $p < 0.005$.

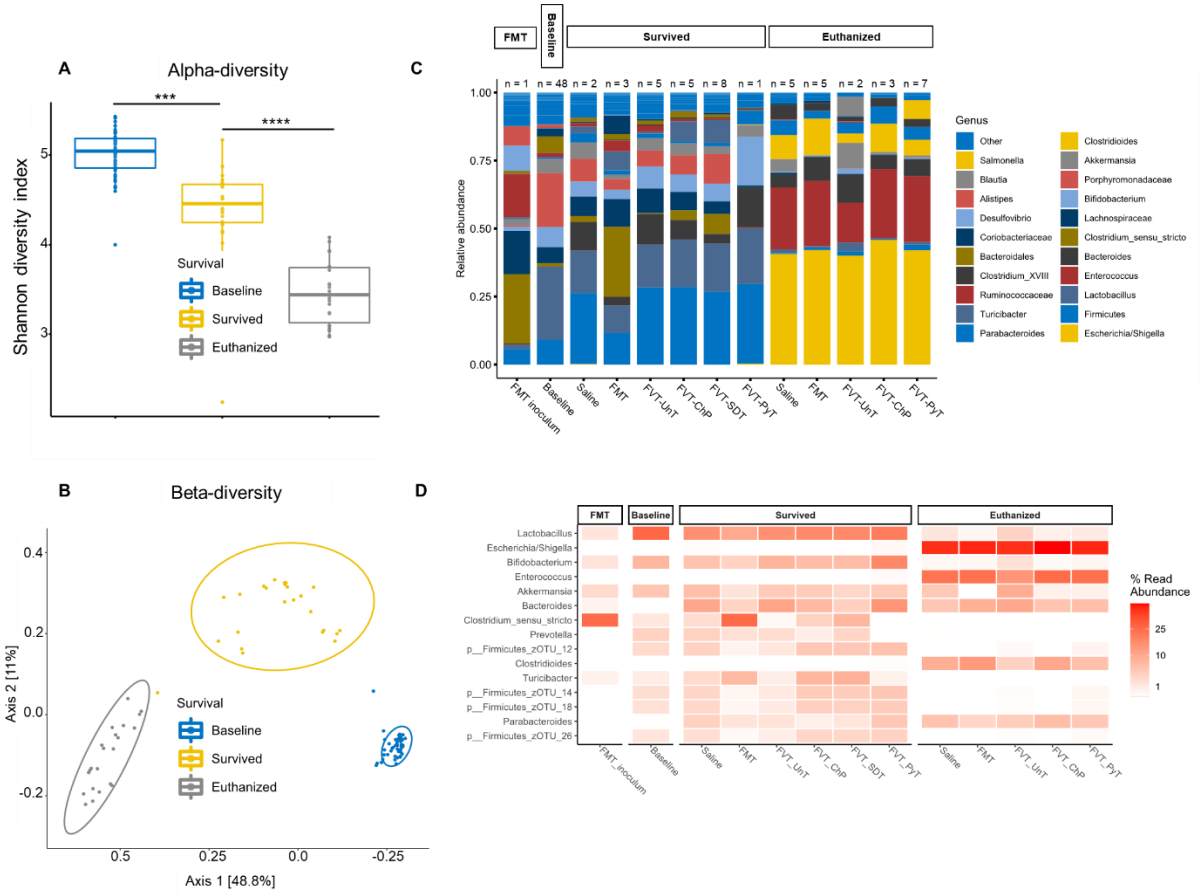

741

742 Fig.4: Bacteriome analysis based on 16S rRNA gene amplicon sequencing. A) The general bacterial Shannon diversity index
743 (alpha-diversity) and B) bray-curtis dissimilarity based PCoA plot (beta diversity) at baseline (before antibiotic treatment), that was
744 compared with the mice that had survived *C. difficile* infection regardless of the treatment and the euthanized mice. C) Barplot and
745 D) heatmap illustrating the bacterial relative abundance of the dominating bacterial taxa that was associated to the different mice
746 that either survived the infection or were euthanized. The number above the bar plots highlight the number of mice of which the
747 taxonomical average was based on. *** = $p < 0.005$. **** = $p < 0.0005$.
748

749

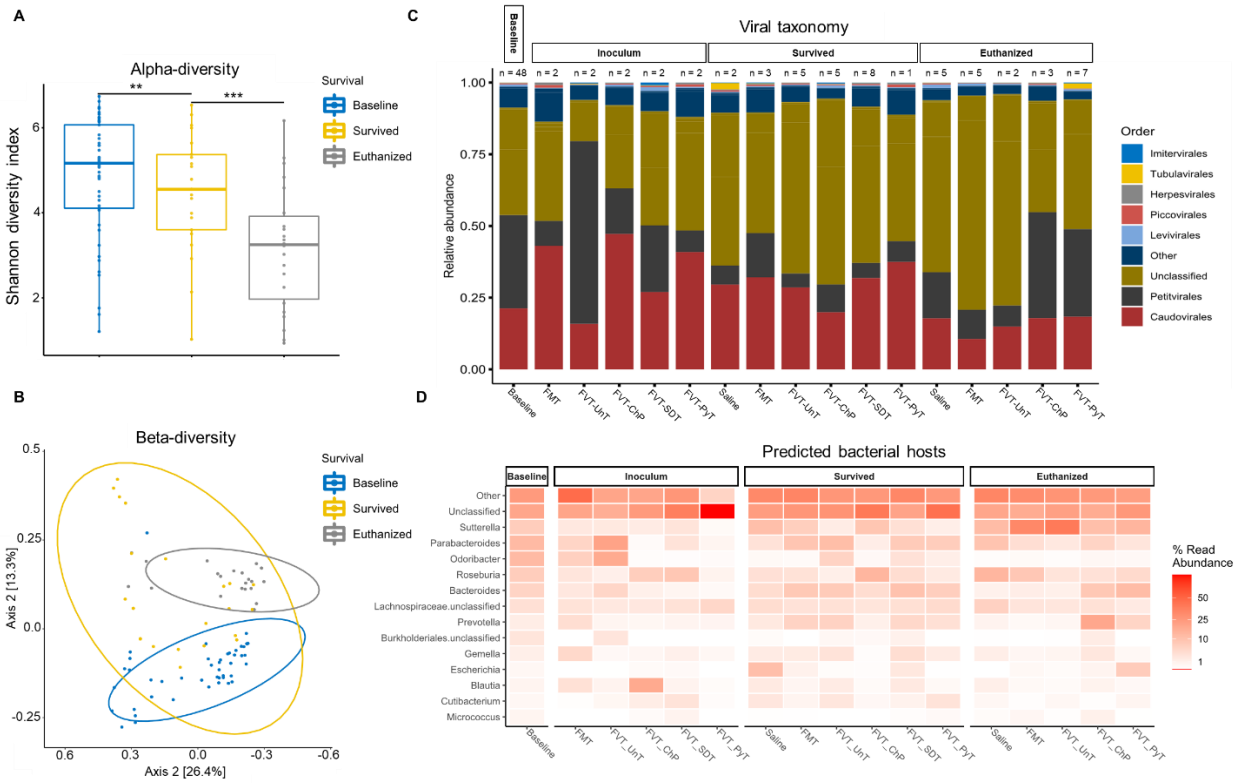

Fig. 5: Metavirome analysis based on whole-genome sequencing. A) The viral Shannon diversity index (alpha-diversity) and B) bray-curtis dissimilarity based PCoA plot (beta diversity) at baseline (before antibiotic treatment), that was compared with the mice that had survived *C. difficile* infection regardless of the treatment and the euthanized mice. C) Barplot showing the relative abundance of the viral taxonomy, and D) heatmap illustrating the relative abundance of the bacterial hosts that are predicted on the basis of the viral sequences. The number above the bar plots highlight the number of mice of which the taxonomical average was based on. ** = $p < 0.01$, *** = $p < 0.005$.

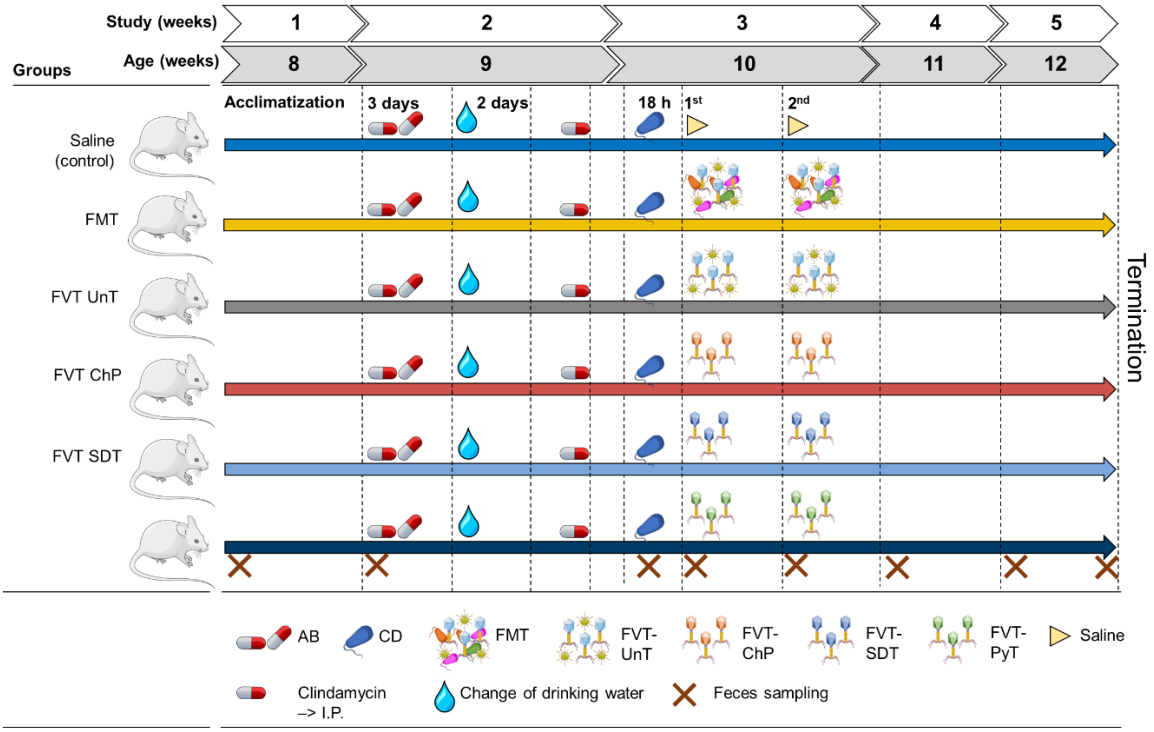

Fig. 6: Overview of the animal model. The mice were initially treated with an antibiotic mixture in their drinking water, intraperitoneal (I.P.) injection of clindamycin and then inoculated with *Clostridioides difficile* (~10^4 CFU). Eighteen hours after the mice were treated with either saline (as control), FMT (fecal microbiota transplantation), FVT-UnT (fecal virome transplantation – Untreated, e.i. sterile filtered donor feces), FVT-ChP (FVT-chemostat propagated fecal donor virome to remove eukaryotic viruses by dilution), FVT-SDT (FVT-solvent/detergent treated to inactivate enveloped viruses), and FVT-PyT (FVT-pyronin Y treated to inactivate RNA viruses). Crosses marks time points of feces sampling.